Int. J. Heat Mass Transfer. Vol. 9, pp. 755–772. Pergamon Press 1966. Printed in Great Britain

NONEQUILIBRIUM HYPERSONIC STAGNATION FLOW WITH ARBITRARY SURFACE CATALYCITY INCLUDING LOW REYNOLDS NUMBER EFFECTS†

G. R. INGER‡

Aerospace Corporation, El Segundo, California

(*Received* 10 *September* 1965 *and in revised form* 17 *February* 1966)

Abstract—Dissociated stagnation point flow on highly cooled blunt bodies in a hypersonic stream of air or diatomic gas is considered, including low Reynolds number effects and nonequilibrium chemical reaction throughout the shock layer. An arbitrary atom recombination rate on the surface is allowed. Based on the continuum thin shock layer model of Cheng, it is shown that in many applications the significant gas phase reaction effects occur in a generalized nonequilibrium vorticity-interaction flow regime, including the transition from recombination rate to dissociation rate-controlled behavior. An approximate analytical solution is given for this regime which predicts atom concentrations and nonequilibrium heat transfer within 10 per cent of exact numerical solutions down to shock layer Reynolds numbers of 100.

NOMENCLATURE

A, dissociation rate parameter;
$\bar{c}_p$, frozen specific heat of mixture;
$\mathscr{D}_b$, boundary-layer dissociation rate distribution function;
f, stream function in similarity plane;
F, vortical inviscid flow field function;
h_d, dissociation energy per unit atom mass;
H, total enthalpy;
H_d, $\alpha_{i,e}\, Le\, h_d/\bar{c}_p\, T_{i,e}$;
I_z, I_θ, boundary-layer flow field functions;
$\mathscr{I}_z$, $\mathscr{I}_\theta$, $\mathscr{I}_z^d$, $\mathscr{I}_\theta^d$, boundary-layer reaction rate integrals (equations 46a, 46b);
$\mathscr{I}_{F_{1,2,3}}$, $\mathscr{I}_F^d$, frozen boundary-layer integrals;
k_D, dissociation rate;
k_R, recombination rate $(=k_r' T^\omega)$;
$\mathscr{K}(T)$, equilibrium constant (equation 9);
Le, Lewis number (Pr/Sc);
p, static pressure;
Pr, Prandtl number;
Q_w, nondimensional heat-transfer rate;
r_d, parameter for inviscid reaction effect on boundary layer;
R_b, body nose radius;
R_m, molecular gas constant;
R_u, universal gas constant;
Re_s, shock layer Reynolds number $(\rho_\infty V_\infty R_b/\mu_s)$;
$\mathscr{R}_b$, boundary-layer recombination rate distribution function;
$\mathscr{R}_i$, inviscid flow reaction rate distribution function;
s, pre-exponential temperature-dependence of dissociation rate,
Sc, Schmidt number;
T, static absolute temperature;
T_D, characteristic dissociation temperature $(=h_d/R_m)$;
T_v, characteristic vibrational energy excitation temperature;
V_∞, free stream flow velocity;
$\dot{w}_a$, net atom production rate from chemical reaction;
x, y, physical coordinates along and normal to body, respectively;
z, $\alpha/\alpha_{i,e}$;
Z, $z(0)/z_{F,w}$.

† This work was supported under U.S. Air Force Contract No. AF 04(695)-260.

‡ Member, Technical Staff, Aerodynamics and Propulsion Research Laboratories.

Greek Symbols

α, atom mass fraction;
β_i, inviscid stagnation point velocity gradient;
γ_w, catalytic efficiency of wall surface;
Γ_b, Damköhler number for boundary layer recombination;
Γ_e^*, composite Damköhler number for gas phase and surface reaction;
Γ_i, Damköhler number for inviscid dissociation reaction;
Δ, shock standoff distance;
ζ_w, Damköhler number for catalytic atom recombination on wall;
η, similarity coordinate at stagnation point;
θ, $T/T_{i,e}$;
κ_s, shock velocity slip parameter;
μ, coefficient of shear viscosity;
ρ, density of mixture;
χ, χ_d, inviscid flow reaction rate integrals;
ω, recombination rate temperature-dependence exponent.

Subscripts

e, conditions at edge of boundary layer;
eq, equilibrium shock layer;
F, chemically frozen shock layer;
i, inviscid flow solution;
s, post-shock conditions;
w, conditions in gas at the wall;
∞, free stream conditions.

1. INTRODUCTION

THE PROBLEM of predicting stagnation point heat transfer from nonequilibrium-dissociated shock layers on blunt bodies arises frequently in reentry technology, fundamental experimental studies of reacting gas flows, and in the development of catalytic probes for measuring state properties in highly dissociated gas flows. Numerous solutions [1–8] of this problem have been given for the high Reynolds number limit where nonequilibrium reaction is confined to a thin boundary layer with the surrounding inviscid flow in equilibrium. However, in the aforementioned applications, significant nonequilibrium effects on heat transfer can also occur at low Reynolds numbers where classical boundary-layer theory no longer applies and nonequilibrium flow exists throughout the shock layer. Although there are several numerical solutions that describe this regime [9, 10], the only analytical solutions to have been carried out are restricted to very small degrees of dissociation and negligible recombination rate throughout the shock layer [11, 17].

As is frequently the case with numerical solutions, the available results for the fully-viscous nonequilibrium shock layer problem describe but a few of the many cases encountered in practice. Furthermore, existing solutions are confined to the extremes of either a perfectly catalytic or completely non-catalytic surface, although it is evident from the results that intermediate degrees of surface catalycity can have an significant effect on nonequilibrium heat transfer. These limitations emphasize the desirability of an approximate theory of nonequilibrium viscous stagnation point flow which provides closed-form engineering solutions for gas phase-surface properties such as heat transfer over a wide range of shock layer conditions, including low Reynolds number effects and the simultaneous effects of both homogeneous and heterogeneous reaction. This paper presents such a theory for hypersonic dissociating diatomic gas flows around highly-cooled blunt bodies. In Section 2, the governing equations and boundary conditions are set forth, based on a continuum thin shock layer flow model due to Cheng [10, 12]. In most cases it is observed that nonequilibrium reaction in the shock layer essentially takes place within the realm of a nonequilibrium vorticity-interaction flow regime composed of a boundary layer (which is not necessarily thin) embedded in a region of vortical nonequilibrium inviscid flow. An approximate analytic solution for the nonequilibrium heat transfer in this regime is then presented in Section 3. Finally, applications are discussed in Section 4, including comparisons with numerical solutions and an

evaluation of the effects of finite surface catalycity.

2. FORMULATION OF THE PROBLEM

(a) *Assumptions*

Consider the flow of a nonequilibrium-dissociating gas across the shock layer at the stagnation point of a two-dimensional or axisymmetric blunt body (Fig. 1). The body is regarded as nonablating with a first-order catalytic atom recombination reaction taking place on the surface. The present analysis is based on

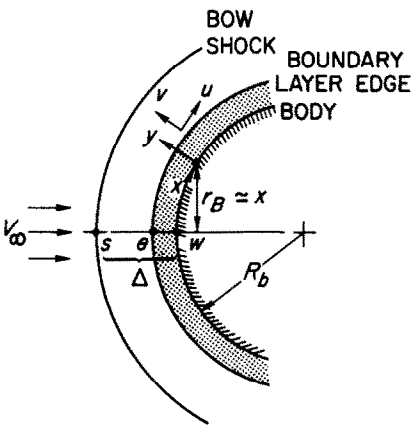

FIG. 1. Flow configuration.

the thin, hypersonic shock layer model of Cheng [10-12]. According to this model, there exists a strong bow shock wave of negligible thickness that is concentric with the body at the stagnation line. Across the shock, the static pressure and normal velocity component are taken to be discontinuous according to the usual Hugoniot relations; however, discontinuities in composition, tangential velocity, and total enthalpy (the so-called "shock slip" effects) are allowed. Between the shock and the body there is assumed a thin ($\Delta/R_b \ll 1$) layer of continuum, viscous reacting gas flow across which the pressure variation is negligible. In this layer, the influence of body curvature and surface slip phenomena is also neglected in comparison to the shock layer vorticity and shock slip effects, when the body is highly cooled.

To simplify the analysis, while retaining the features essential for determining nonequilibrium reaction effects on overall shock layer properties such as heat transfer, the following additional assumptions are made. (1) The gas is, or can be reasonably approximated by, a binary gas mixture composed of atoms (mass fraction α) and molecules. (2) Prandtl number, Schmidt number, and the density–viscosity product are each constant across the shock layer. (3) Thermal diffusion effects are negligible. (4) Excited electronic internal energy states are neglected. (5) The average specific heat of the mixture is a constant. Assumption (1) is exact for a pure diatomic gas and has been shown to be a satisfactory approximation for high temperature air in the absence of ablation products or thermally significant ionization when appropriately averaged thermo-chemical properties are used [1, 7, 9]. The customary simplifying assumptions (2)–(5) likewise have been amply qualified as satisfactory engineering approximations for nonablating, highly cooled blunt bodies unless the finer details of the temperature and composition profiles across the shock layer are of interest [1, 7–10, 13].

(b) *Governing relations*

An important consequence of the thin shock layer model adopted here is that the governing Navier–Stokes flow equations reduce to the familiar parabolic differential equations of boundary-layer theory [10]. Taking advantage of the known self-similar nature of these equations for stagnation point flow, a stream function is introduced

$$\psi = \left(\frac{\rho_R \mu_R \beta_i}{1+\nu}\right)^{\frac{1}{2}} x^{\nu+1} f(\eta) \begin{Bmatrix} \nu = 0, \text{two-dim.} \\ \nu = 1, \text{axisymm} \end{Bmatrix} \quad (1)$$

in terms of the similarity coordinate

$$\eta = \left[\frac{(1+\nu)\beta_i}{\rho_R \mu_R}\right]^{\frac{1}{2}} \int_0^Y \rho \, dY \quad (2)$$

where β_i is defined as the *inviscid* stagnation point velocity gradient and $\rho_R \mu_R$ is evaluated at an appropriately chosen reference condition in

the shock layer. Then, using the above assumptions and writing $p(y) = \text{constant} = p_{i,w}$, $dp/dx = -\rho_{i,w}\beta_i^2 x$ with the subscript i denoting the inviscid solution, the governing flow equations of momentum, atomic specie mass, and energy conservation, respectively, are

$$ff'' + f''' = (1 + \nu)^{-1}\left(f'^2 - \frac{\rho_{i,w}}{\rho}\right) \quad (3)$$

$$Sc\, f\alpha' + \alpha'' = -\frac{Sc}{(1 + \nu)\beta_i}(\dot{w}_a/\rho) \quad (4)$$

$$Pr\, fH' + H'' + (Le - 1)h_d\alpha'' = 0 \quad (5)$$

where a prime denotes differentiation with respect to η, h_d is the dissociation energy per unit atom mass, and $\dot{w}_a/\rho$ is the net rate of atom production from homogeneous chemical reaction as given below. The local total enthalpy H is given in the strong shock approximation

$$H \simeq \bar{c}_p T + \alpha h_d. \quad (6)$$

By virtue of equations (4) and (6), the energy equation (5) can be rewritten in the following form involving T explicitly, which proves useful later:

$$Pr\, fT' + T'' = \frac{Pr\, h_d}{(1 + \nu)\beta_i \bar{c}_p}(\dot{w}_a/\rho). \quad (7)$$

There is considered here a mixture of atoms and molecules undergoing the dissociation–recombination reaction

$$A_2 + X \underset{k_R}{\overset{k_D}{\rightleftharpoons}} 2A + X$$

where A_2, A, and X denote a molecule, atom and any third body collision partner, respectively. For this reaction, application of the laws of phenomenological chemical kinetics and mass action plus the equation of state $p = \rho R_m(1 + \alpha)T$ yields

$$\frac{\dot{w}_a}{\rho} = 4k_R' T^{\omega}(p/R_u T)^2\left[\frac{(1 - \alpha)\mathscr{K}(T)}{4p} - \frac{\alpha^2}{1 + \alpha}\right] \quad (8)$$

where the equilibrium constant $\mathscr{K}(T) \equiv R_u T k_D/k_R$ may be represented by [7, 9]

$$\mathscr{K}(T) \simeq AT^s(1 - \exp[-T_v/T])\exp[-T_D/T]. \quad (9)$$

In equations (8) and (9), $k_R = k_R' T^{\omega}$ is an averaged recombination rate for the mixture, ω, A and s are constants, $T_D \equiv h_d/R_m$ and T_v is a characteristic temperature for molecular vibrational energy excitation. (Specific values of the various thermochemical parameters employed are cited later.) The two terms on the right-hand side of equation (8) represent the effect of dissociation and recombination, respectively. They are exactly equal in the limiting case of equilibrium-dissociating flow, where equation (4) becomes superfluous.

Low Reynolds number effects enter the present formulation explicitly through the outer boundary conditions at the shock wave. Allowing for shear, heat conduction and diffusion behind the bow shock in the manner described by Cheng [10, 12], conservation of tangential momentum, atomic specie mass, and total energy across the shock surface at $\eta = \eta_s$ yields

$$f'(\eta_s) = V_\infty/\beta_i R_b - \frac{\rho_s\mu_s}{\rho_R\mu_R}[f''(\eta_s)/f_s] \quad (10)$$

$$\alpha(\eta_s) \equiv \alpha_s = \alpha_\infty - \frac{\rho_s\mu_s}{\rho_R\mu_R}[\alpha'(\eta_s)/s_c f_s] \quad (11)$$

$$H(\eta_s) = H_\infty - \frac{\rho_s\mu_s}{\rho_R\mu_R} \times \left[\frac{H'(\eta_s) + (Le - 1)h_d\,\alpha'(\eta_s)}{Pr\, f_s}\right] \quad (12)$$

where $H_\infty = \alpha_\infty h_d + \frac{1}{2}(V_\infty^2)$ in the strong shock approximation. The last terms in each of these equations constitute jumps (or slip) in tangential velocity, concentration, and total enthalpy across the shock due to the post-shock gradients in these quantities. It is seen that the shock transition is non-adiabatic when the last term in equation (12) becomes comparable to the free stream total energy.

Now, an additional boundary condition is required since the shock location η_s is unknown in the general case. This is supplied by a mass

conservation statement across the bow shock at the stagnation line in the similarity variables, which yields

$$f(\eta_s) \equiv f_s = \left[\frac{\rho_s \mu_s}{\rho_R \mu_R}\left(\frac{\rho_\infty/\rho_s}{1+v}\right)\frac{V_\infty}{\beta_i R_b}\right]^{\frac{1}{2}} Re_s^{\frac{1}{2}} \qquad (13)$$

In the high Reynolds number limit of boundary-layer flow, where the shock is considered infinitely far from the body, one may discard equation (13) and neglect the shock slip terms in equations (10)–(12).

The inner boundary conditions at the body surface are

$$f(0) = f'(0) = 0 \qquad (14)$$

$$T(0) = T_w \quad \text{(given)} \qquad (15)$$

$$H(0) = H_w = \bar{c}_p T_w + \alpha(0)\, h_d \qquad (16)$$

$$\alpha'(0) = \frac{Sc\, K_w}{\mu_w}\left[\frac{\rho_R \mu_R}{(1+v)\beta_i}\right]^{\frac{1}{2}} \alpha(0) \equiv \zeta_w\, \alpha(0) \qquad (17)$$

In equation (17), K_w is the speed of catalytic atom recombination on the surface, a known function of T_w, wall material, and the particular gas; it is related to the catalytic efficiency γ_w by $\gamma_w = K_w(\pi/R_m T_w)^{\frac{1}{2}}$. The parameter ζ_w is the Damköhler number for heterogeneous reaction; when $\zeta_w \to \infty$, the surface is completely catalytic [$\alpha(0) = 0$], whereas $\zeta_w = 0$ implies that the surface is perfectly non-catalytic [$\alpha'(0) = 0$]. Once the governing equations are solved, the surface heat-transfer rate $\dot{q}_w$ is computed from either of the two relations

$$\left[\frac{\rho_R \mu_R}{(1+v)\beta_i}\right]^{\frac{1}{2}} \frac{Pr\, \dot{q}_w}{\mu_w} \equiv Q_w = H'(0) + (Le - 1)h_d\, \alpha'(0) \qquad (18a)$$

$$= \bar{c}_p\, T'(0) + Le\, h_d\, \alpha'(0) \qquad (18b)$$

(c) *Some important physical features*

It is clear that exact solutions to the foregoing nonlinear boundary value problem must be carried out numerically on a digital computer. However, by examining some results of existing numerical studies, one can devise a simplified theoretical model of the problem which applies throughout the entire nonequilibrium flow regime occurring in most applications.

Consider Fig. 2, where the nondimensional shock standoff distance obtained by various

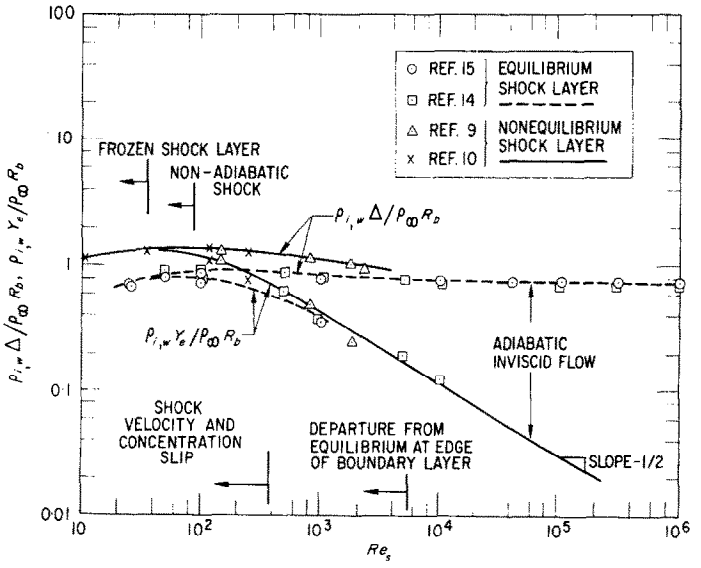

FIG. 2. Nonequilibrium stagnation shock layer properties.

investigations [9, 10, 14, 15] for highly-cooled bodies is plotted versus Reynolds number. Also shown is the corresponding nondimensional thickness y_e/R_b of that part of the shock layer near the wall which contains 99 per cent of the enthalpy variation across the shock layer. Indicated on the graph are the Reynolds numbers where velocity and total enthalpy shock slip become important, plus the lowest Reynolds numbers at which appreciable departure from equilibrium at Y_e and chemical freezing of the flow throughout the shock layer occur for $R_b \leqslant 3$ ft and $V_\infty \leqslant 25000$ ft/s. Now it can be seen from Fig. 2 that there is a distinct region of essentially adiabatic flow adjacent to the shock throughout most of the nonequilibrium-dissociating shock layer regime. That is, when the Reynolds number is low enough that the entire shock layer flow is fully viscous and a nonadiabatic shock transition (total enthalpy shock slip) occurs, this flow has become almost completely chemically frozen throughout. Figure 2 also indicates the well-known fact that the physical shock standoff distance is relatively insensitive to Reynolds number when the shock wave is adiabatic, while the corresponding enthalpy sublayer (boundary layer) thickness grows as $Re_s^{-\frac{1}{2}}$. In contrast, the opposite situation is true in the similarity plane, where the shock distance (in terms of f) varies as $Re_s^{\frac{1}{2}}$ while the outer edge f_e of the enthalpy sublayer remains essentially fixed until f_s approaches f_e closely.

It should be pointed out that the *adiabatic* flow region identified above can also be taken to be one of inviscid (albeit vortical) flow, while retaining velocity and concentration slip terms in the boundary conditions (10) and (11). This can be shown by a detailed analysis of the governing equations [16] and is corroborated by numerical results [10].

The foregoing observations suggest that for nose radii on the order of a foot or less and flight speeds $V_\infty \lesssim 25000$ ft/s (or total enthalpies equivalent thereto), the nonequilibrium stagnation point heat-transfer problem in air or airlike-gases can be conveniently broken down into two successive flow regimes. The first, and most important, ranges from the usual high Reynolds number situation of a thin boundary layer surrounded by an equilibrium-dissociated inviscid shock layer down to values of $Re_s \approx 10^2$ where the shock layer becomes almost-fully viscous with nearly chemically-frozen flow throughout. In this regime, which is the subject of the present paper, there exists an outer region of vortical, nonequilibrium inviscid shock layer flow surrounding an inner (but not necessarily thin) boundary layer. The second regime at lower Reynolds numbers involves a fully viscous nonadiabatic shock layer flow with appreciable slip in total enthalpy (as well as velocity and concentration) behind the shock. Here, the gas phase reaction effects may be taken as small perturbations on a frozen flow solution and the recombination rate neglected throughout the shock layer. Analytical solutions to this problem that include shock slip effects have been given by Inger [16] and Buckmaster [17].

3. APPROXIMATE SOLUTION FOR THE GENERALIZED VORTICITY-INTERACTION REGIME

We shall proceed by obtaining an approximate closed form solution for the boundary-layer region (allowing for reaction therein) and matching it with a corresponding nonequilibrium inviscid flow solution. This approach is similar to Cheng's vorticity interaction theory [12] for a perfect gas, generalized here to include the effects of nonequilibrium reaction throughout the shock layer, arbitrary surface catalycity and first-order velocity, concentration and temperature shock slip effects based on the inviscid flow gradients.

(a) *Outer inviscid flow region*

Consider first the inviscid nonequilibrium flow in the region $f_e \leqslant f \leqslant f_s$. This flow is governed by equations (3) to (5) with the highest order derivatives of α and f dropped, plus the following integral of the energy equation for

adiabatic conditions:

$$H_i(\eta) \simeq H_\infty \simeq \bar{c}_p T_i(\eta) + \alpha_i(\eta) h_d \quad (19)$$

The boundary conditions at the shock are given by equations (10) and (11), respectively, whereas only the single boundary condition $f_i(0) = 0$ from equation (14) is to be applied at the body surface.

The inviscid momentum equation, viewed as a first-order differential equation in $f_i'^2$ with f_i as the independent variable, can be integrated directly with the use of equation (10) to

$$f_i'^2 = \frac{\rho_{i,w}}{\rho_i} + f_i^{2/(1+\nu)} \left[C - \rho_{i,w} \int_{f_s}^{f_i} \frac{\mathrm{d}\rho_i/\mathrm{d}f}{\rho_i^2 f^{2/(1+\nu)}} \mathrm{d}f \right] \quad (20)$$

where

$$C = \frac{f'_{i,0}(\eta_s)}{\kappa_s} + \frac{f_s^{2/(1+\nu)}}{2\kappa_s^2} \left\{ 1 - \left[1 + \frac{4\rho_{i,w}\kappa_s^2}{\rho_{i,s} f_s^{4/(1+\nu)}} + \frac{4 f'_{i,0}\kappa_s}{f_s^{2/(1+\nu)}} \right]^{\frac{1}{2}} \right\} \quad (21)$$

with $f'_{i,0}(\eta_s) \equiv V_\infty/\beta_i R_b$ and $\kappa_s \equiv \rho_s \mu_s/(1+\nu)\rho_R \mu_R f_s^{2\nu/(1+\nu)}$. Equation (20) generalizes the velocity-stream function relationship given in Hayes and Probstein [18] for a hypersonic, vortical, constant density shock layer flow to the case where nonequilibrium reaction is present. [The density integral term introduces the chemical reaction effect; it can be dropped in the strong shock approximation for either chemically frozen flow ($\rho_i = \rho_{i,s}$) or equilibrium flow ($\rho_i = \rho_{i,\mathrm{eq}} = \rho_{i,w}$).] Now, the primary interest here lies in determining $\alpha_i(f_i)$ and $T_i(f_i)$ rather than the velocity field. Since the effect of chemical reaction on these profiles depends only weakly on the details of the velocity distribution [19], the effect of chemical reaction on $f_i'(\eta)$ may be neglected to a first approximation by taking $\rho_i = \rho_{i,s}$ in equation (20); thus we obtain

$$f_i'(\eta) \simeq \left[\frac{\rho_{i,w}}{\rho_{i,s}} + C f_i(\eta)^{2/(1+\nu)} \right]^{\frac{1}{2}}$$

An analytical solution of equations (4) (with α'' dropped), (8) and (19) for the inviscid atom concentration and temperature distributions can now be obtained by adapting a technique due to Gibson and Sowyrda [19]. For this purpose, it is convenient to nondimensionalize T with respect to T_D and thus rewrite these equations as

$$f_i\alpha_i' = -\mathscr{R}_i\Gamma_i \equiv -\left[(1-\alpha_i) \left(\frac{T_i}{T_D} \right)^{\omega+s-2} (1 - \exp[-T_v/T_i]) \exp[-T_D/T_i] - \frac{4p}{\mathrm{A} T_D^s} \left(\frac{T_i}{T_D} \right)^{\omega-2} \frac{\alpha_i^2}{1+\alpha_i} \right] \Gamma_i \quad (23)$$

$$T_i/T_D = (R_m/\bar{c}_p)[(H_\infty/h_d) - \alpha_i] \quad (24)$$

where $\mathscr{R}_i$ is a net reaction rate distribution function composed of contributions from dissociation and recombination, respectively, and

$$\Gamma_i = \frac{k' A T_D^{\omega+s} p}{(1+\nu)(R_u/T_D)^2 \beta_i} \quad (25)$$

is a characteristic (flow time/dissociation time) ratio for the inviscid flow. Since equation (24) allows $\mathscr{R}_i$ to be expressed as a function of α_i alone, equation (23) may be regarded as a separable first order differential equation and thus integrated using boundary condition (11) to obtain the following implicit solution:

$$\chi(\alpha_i) = \chi(\alpha_{i,s}) + \Gamma_i F(f_i) \quad (26)$$

where

$$\chi(\alpha_i) \equiv \int_0^{\alpha_i} \mathscr{R}_i^{-1}(\alpha)\, \mathrm{d}\alpha,$$

$$\alpha_{i,s} = \alpha_\infty + [\rho_s \mu_s \Gamma_i \mathscr{R}_i(\alpha_{i,s})/\rho_R \mu_R Sc f_s^2]$$

and

$$F(f_i) \equiv \int_{f_i}^{f_s} (ff')^{-1}\, \mathrm{d}f.$$

A detailed study [19] of the function $\chi(\alpha_i)$ for the Lighthill ideal dissociating gas model [20] has shown that the effect of recombination may be neglected until α_i is quite close to the equilibrium value $\alpha_{i,w}$ attained at the body ($f_i = 0$).

Consequently, it is possible to accurately approximate $\chi(\alpha_i)$ by

$$\chi(\alpha_i) \simeq -\chi_d(\alpha_{i,w}) \ln\left[1 - \frac{\chi_d(\alpha_i)}{\chi_d(\alpha_{i,w})}\right] \quad (27)$$

where $\chi_d(\alpha_i)$ is the value of $\chi(\alpha_i)$ with the recombination rate term neglected. The dissociation rate function $\chi_d(\alpha_i)$ is plotted in Figs. 3(a) and 3(b) for typical values of the three parameters $\bar{c}_p/R_m$, H_∞/h_d and $\omega + s$. It is seen that this function is quite sensitive to both the recombination rate temperature exponent ω and the characteristic temperature ratio T_v/T_D.

The function $F(f_i)$ can be expressed in the following closed form when approximation (22) is used:

$$F(f_i) \simeq \left(\frac{1+\nu}{2}\right)\left(\frac{\rho_{i,s}}{\rho_{i,w}}\right)^{\frac{1}{2}} \ln \times \left(\frac{\left[1 + \bar{C} f_i^{2/(1+\nu)}\right]^{\frac{1}{2}} + 1}{\left[1 + \bar{C} f_i^{2/(1+\nu)}\right]^{\frac{1}{2}} - 1}\right) \times \left(\frac{\left[1 + \bar{C} f_s^{2/(1+\nu)}\right]^{\frac{1}{2}} - 1}{\left[1 + \bar{C} f_s^{2/(1+\nu)}\right]^{\frac{1}{2}} + 1}\right) \quad (28)$$

where $\bar{C} \equiv \rho_{i,s}\, C/\rho_{i,w}$. We note that $F(f_i)$ is logarithmically infinite at $f_i = 0$, reflecting the fact that the *local* inviscid flow time becomes infinite at the body. This is consistent with equation (26), since it correctly implies that $\chi \to \infty$ and hence $\mathscr{R}_i \to 0$ and $\alpha_i \to \alpha_{i,w}$ as $f_i \to 0$ for all values of Γ_i.

The foregoing solution affords a relatively simple analytical determination of the nonequilibrium inviscid flow properties. One first establishes the post-shock conditions by an iterative calculation (which is unnecessary if shock slip effects are neglected), starting with the known conditions for zero slip. The first approximation for $\alpha_{i,s} - \alpha_\infty$ so obtained is usually sufficient in practice. One then can obtain $\chi(\alpha_i)$ as a function of f_i from equations (26) and (28) and thus find $\alpha_i(f_i)$ and $T_i(f_i)$ from equation (27), Fig. 3, and equation (24). It is noted that the present nonequilibrium inviscid flow solution possesses the important property of binary scaling [21] throughout that portion of the shock layer where recombination can be neglected.

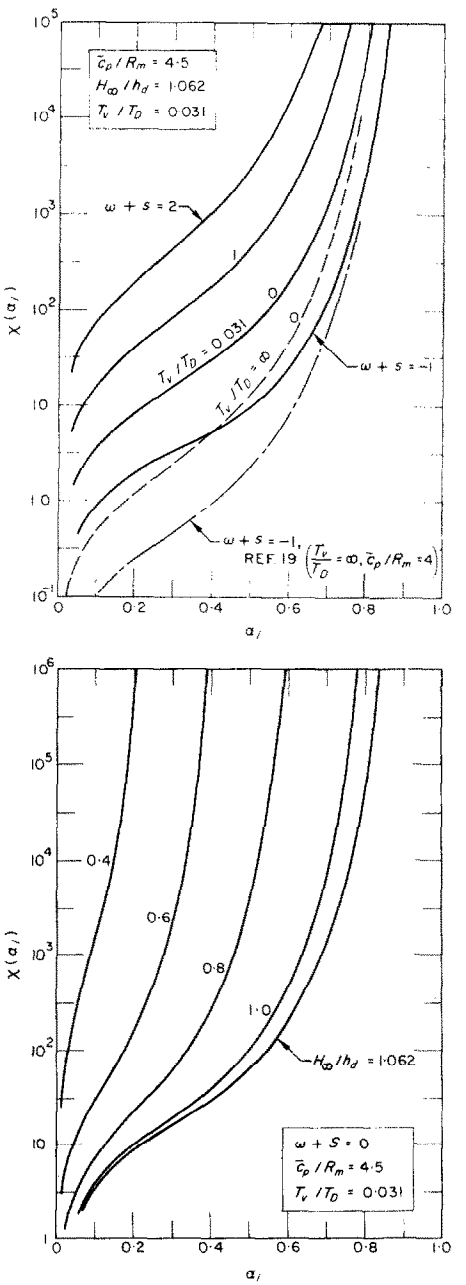

FIG. 3. Inviscid dissociation rate integral $\chi_d(\alpha_i)$.
(a) Effect of $\omega + s$.
(b) Effect of H_∞/h_d.

(b) *Inner boundary-layer region*

Here, we must solve equations (3), (4) and (8) as they stand subject to all the wall boundary conditions (14) to (17). The outer boundary conditions are determined by matching with the foregoing inviscid solution in the following way. To the order of approximation involved in the present generalized vorticity interaction model, each of the dependent variables f', α and T at the outer edge f_e of the boundary layer must be equal to the corresponding inviscid flow values at the same value of the stream function $f_i = f_e$ [18]. (It can be shown through detailed analysis that this procedure also insures matching of the gradients in velocity, atom concentration and temperature when the nonequilibrium state of the inviscid flow is taken into account [16].)

To the same order of approximation and in keeping with the earlier discussion of Fig. 2, f_e is determined as follows. When $f_s \geqslant f_e$, f_e is taken to be independent of Reynolds number and equal to the value of f at $H/H_e = 0{\cdot}99$ given by stagnation point boundary layer theory [22, 23]. The values of f_e obtained in this way, which essentially depend only on the Prandtl number for highly-cooled walls ($H_w/H_e \lesssim 0{\cdot}20$) if the even number is of order unity, are given in Table 1. On the other hand, at sufficiently low Reynolds numbers where one would predict f_s to be less than f_e, we assume $f_e = f_s$. As shown below, this sequence of approximation affords a good account of nonequilibrium heat transfer down to Reynolds numbers where relatively little dissociation effects remain in the shock layer.

To facilitate an analytical solution, the boundary-layer velocity profile may be approximated by a perfect gas solution (e.g. reference [12]) relative to conditions at the outer edge. This is consistent with our treatment of the velocity field in the outer inviscid flow region. Moreover, it is justified by the fact that the solutions to the boundary layer energy and specie conservation equations for a highly cooled wall are not significantly affected by the effect of chemical reaction on the velocity profile when overall properties such as heat transfer are of interest [3, 7, 9].

The solution proceeds in a manner similar to the analysis of reference [7], taking care here to account for the presence of a nonequilibrium, vortical inviscid flow at the edge of the boundary layer. Thus, by introducing the new dependent variables $z \equiv \alpha/\alpha_{i,e}$, $\theta \equiv T/T_{i,e}$ and using equations (8) and (9) evaluated at $f = f_e$ to express $\mathscr{K}(T_e)/p$ in terms of $(\dot{w}_a/\rho)_e$ and $\alpha_{i,e}^2/(1 + \alpha_{i,e})$, equations (4) and (7) can be rewritten as

$$Sc\, f Z' + Z'' = \frac{\alpha_{i,e}\, \Gamma_b\, \mathscr{R}_b(z, \theta)}{1 + \alpha_{i,e}} - \frac{Sc\, \Gamma_i}{\alpha_{i,e}}\, \mathscr{R}_i(\alpha_{i,e})\, \mathscr{D}_b(z, \theta) \quad (29)$$

$$Pr f \theta' + \theta'' = - H_d(Sc f Z' + Z'') \quad (30)$$

where

$$\Gamma_b = \frac{4\, Sc\, k_R'\, T_{i,e}^{\omega}(p/R_u\, T_{i,w})^2}{(1 + \nu)\, \beta_i} \quad (31)$$

is the characteristic (flow time/recombination time ratio) for the stagnation boundary layer [1, 7], $H_d \equiv \alpha_{i,e}\, Le\, h_d/\bar{c}_p\, T_{i,e}$ and

$$\mathscr{R}_b(z, \theta) = \left(\frac{1 + \alpha_{i,e}}{1 + \alpha_{i,e} z}\right) \theta^{\omega - 2} \left\{ z^2 - \left(\frac{1 - \alpha_{i,e}^2 z^2}{1 - \alpha_{i,e}^2}\right)\left(\frac{1 - \exp[-\theta_v/\theta]}{1 - \exp[-\theta_v]}\right) \times \exp[-(\theta_d/\theta) + \theta_d] \right\} \quad (32)$$

$$\mathscr{D}_b(z, \theta) = \left(\frac{1 - \alpha_{i,e} z}{1 - \alpha_{i,e}}\right) \theta^{\omega + s - 2} \times \left(\frac{1 - \exp[-\theta_v/\theta]}{1 - \exp[-\theta_v]}\right) \times \exp[-(\theta_d/\theta) + \theta_d] \quad (33)$$

The function $\mathscr{R}_b$, which vanishes at $f = f_e (z = \theta = 1)$, represents the net reaction rate distribution across the boundary layer than would exist *if* the inviscid flow was in equilibrium [$\mathscr{R}_i(\alpha_{i,e}) = 0$] at f_e. The recombination rate ($\sim z^2$) near the surface is the major contribution to this function

across the layer for a highly cooled wall, the contribution of the opposing exponential dissociation rate term being confined to the region near the outer edge. The function $\mathscr{D}_b$ represents the effect of the nonequilibrium dissociation rate in the inviscid flow, as carried into the boundary layer and modified by the sharply decreasing velocity and temperature therein. For a highly cooled wall where the dissociation rate quenches rapidly across the boundary layer, $\mathscr{D}_b \ll \mathscr{R}_b$ except in the relatively hot gas region near the outer edge. Consequently, this "carry-over" effect has a negligible influence on the gas properties near the surface when $\Gamma_b \gtrsim \Gamma_i \mathscr{R}_i(\alpha_{i,e})/\alpha_{i,e}$, where the situation is completely controlled by the recombination rate near the wall. However, at sufficiently low ambient densities where appreciable departure from equilibrium in the inviscid flow occurs together with a rapid freezing out of recombination near the wall [$\Gamma_b \ll \Gamma_i \mathscr{R}_i(\alpha_{i,e})/\alpha_{i,e}$], the *inviscid* dissociation rate becomes the controlling factor in determining the surface properties.

Relations governing conditions in the gas at the wall can be obtained by performing formal double integrations of equations (29) and (30). Carrying these out and applying the boundary conditions, one finds

$$Z \equiv \frac{z(0)}{z_{F,w}} = \frac{z'(0)}{z'_{F,w}} = 1 - \frac{\alpha_{i,e}\,\Gamma_b\,\mathscr{I}_z(f_e)}{1+\alpha_{i,e}} + \frac{Sc\,\Gamma_i}{\alpha_{i,e}}\mathscr{R}_i(\alpha_{i,e})\mathscr{I}^d_z(f_e) \quad (34)$$

$$I_\theta(f_e)\,\theta'(0) = 1 - \theta_w + H_d(1-Z)\frac{\mathscr{I}_\theta(f_e)}{\mathscr{I}_z(f_e)} + H_d\frac{Sc\,\Gamma_i\,\mathscr{R}_i(\alpha_{i,e})}{\alpha_{i,e}}\mathscr{I}^d_z(f_e)\left[\frac{\mathscr{I}_\theta(f_e)}{\mathscr{I}_z(f_e)} - \frac{\mathscr{I}^d_\theta(f_e)}{\mathscr{I}^d_z(f_e)}\right] \quad (35)$$

where

$$\mathscr{I}_z(f_e) \equiv \int_0^{\eta(f_e)} \exp\left[-Sc\int_0^\eta f\,d\eta\right]\left\{\int_0^\eta \exp\left[Sc\int_0^\eta f\,d\eta\right]\mathscr{R}_b\,d\eta\right\}d\eta \quad (36a)$$

$$\mathscr{I}^d_z(f_e) \equiv \int_0^{\eta(f_e)} \exp\left[-Sc\int_0^\eta f\,d\eta\right]\left\{\int_0^\eta \exp\left[Sc\int_0^\eta f\,d\eta\right]\mathscr{D}_b\,d\eta\right\}d\eta \quad (36b)$$

$$I_z(f_e) \equiv \int_0^{\eta(f_e)} \exp\left[-Sc\int_0^\eta f\,d\eta\right]d\eta \quad (36c)$$

and where $\mathscr{I}_\theta(f)$, $\mathscr{I}^d_\theta(f)$ and $I_\theta(f)$ are obtained from equations (36) by replacing Sc with Pr in the exponential terms involving $\int_0 f\,d\eta$. The functions $z_{f,w}$ and $z'_{f,w}$ corresponding to frozen shock layer flow are given by

$$z_{F,w} = \zeta_w^{-1} \qquad z'_{F,w} = [1+\zeta_w I_z(f_e)]^{-1} \quad (37)$$

It is noted that the ratios $\mathscr{I}_\theta(f_e)/\mathscr{I}_z(f_e)$ and $\mathscr{I}^d_\theta(f_e)/\mathscr{I}^d_z(f_e)$ are exactly equal to unity for $Le = 1$ regardless of the magnitude of the reaction rates or the Reynolds number. Furthermore, for highly cooled walls, they are very weak functions of Le alone when $0{\cdot}5 \lesssim Le \lesssim 2$ [7]. Since the last term in equation (35) therefore vanishes identically for $Le = 1$ and is usually negligible compared to unity otherwise, it will henceforth be neglected.

We can now solve equation (34) for Z, considering the simultaneous effects of gas phase and catalytic surface reaction, as follows. By recognizing that the major contribution of the function $\mathscr{R}_b(z,\theta)$ to the integral $\mathscr{I}_z(f_e)$ for highly cooled walls derives from the recombination rate near the surface regardless of the surface catalycity, it is possible to accurately approximate $\mathscr{I}_z(f_e)$ and $\mathscr{I}^d_z(f_e)$ by the simplified expressions [7]

$$\mathscr{I}_z(f_e) \simeq \left[\frac{1+\alpha_{i,e}}{1+\alpha_{i,e}\,z(0)}\right]z^2(0)\left[\mathscr{I}_{F1} + 2\,\zeta_w I_z(f_e)\,\mathscr{I}_{F_2} + \zeta_w^2 I_z^2(f_e)\,\mathscr{I}_{F_3}\right] \quad (38a)$$

$$\mathscr{I}^d_z(f_e) \simeq \mathscr{I}^d_F \quad (38b)$$

where $\mathscr{I}_{F_{1,2,3}}$ and $\mathscr{I}^d_F$ are reaction rate integrals based on the known frozen flow solution [values are given in the Appendix along with $I_z(f_e)$]. Since the underlying physical arguments and simplifications leading to equation (38)

essentially depend only on the highly cooled wall assumption (see reference 7 for a detailed discussion), these approximations may also be used in the present problem *provided*: (1) conditions at $f = f_e$ based on the nonequilibrium inviscid flow solution (rather than equilibrium inviscid flow values) are used in evaluating the parameters θ_w, θ_d, H_d, Γ_b and Γ_i; (2) a vorticity-interaction solution for the boundary layer velocity profile is used in evaluating the functions (36). Then, substituting equation (38) into equation (34) and solving the resulting quadratic in Z we obtain

$$\frac{Z}{1+r_d} = \frac{\{1+\alpha_{i,e}\,z_{F,w}(1+r_d)]^2 + 4\,(1+r_d)\,\Gamma^*\}^{\frac{1}{2}} - [1-\alpha_{i,e}\,z_{F,w}(1+r_d)]}{2[\alpha_{i,e}\,z_{F,w}(1+r_d) + (1+r_d)\,\Gamma^*]} \tag{39}$$

where

$$r_d \equiv \frac{Sc\,\Gamma_i\,\mathscr{R}_i(\alpha_{i,e})\,\mathscr{I}_F^d}{\alpha_{i,e}} \tag{40}$$

represents explicitly the "carry-over" effect of the nonequilibrium dissociation rate at the edge of the boundary layer and

$$\Gamma^* \equiv \alpha_{i,e}\,\Gamma_b\,\frac{\mathscr{I}_{F_1} + 2\,\zeta_w\,I_z(f_e)\,\mathscr{I}_{F_2} + \zeta_w^2\,I_z^2(f_e)\,\mathscr{I}_{F_3}}{[1+\zeta_w\,I_z(f_e)]^2} \tag{41}$$

is a composite Damköhler number for combined gas phase and catalytic surface recombination reaction. In Fig. 4, $Z/(1+r_d)$ is plotted as a function of $(1+r_d)\,\Gamma^*$ for different values of the parameter $\alpha_{i,e}\,z_{F,w}\,(1+r_d)$. It is seen that this parameter has a small effect when less than unity, in which case $Z/(1+r_d)$ becomes a universal function of $(1+r_d)\,\Gamma^*$ alone regardless of the individual homogeneous or heterogeneous reaction rates.

When the inviscid flow is in equilibrium ($r_d = 0$), equation (39) reduces to precisely the result given in reference [7]. On the other hand, when there is a significant departure from equilibrium at the edge of the boundary layer and the inviscid dissociation rate is the controlling gas phase reaction [$\Gamma^* \ll 1$, $r_d \gtrsim 0(1)$], we find

$$Z \simeq 1 + r_d \tag{42}$$

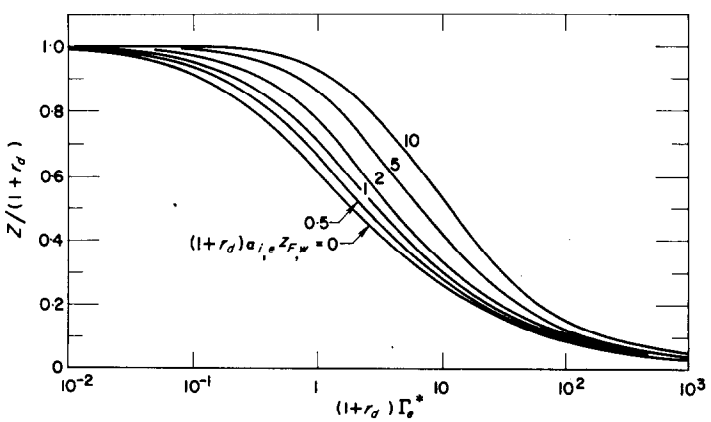

FIG. 4. Universal nonequilibrium boundary layer atom concentration solution.

Since $r_d \sim p/\beta_i \sim \rho_\infty R_b$ for fixed ambient gas properties and free-stream velocity, equation (42) implies that binary scaling holds in the boundary layer, as would be expected for negligible recombination.

Using equations (34) and (35), the nonequilibrium heat transfer can now be expressed in terms of Z. To do this, we identify

$$[I_\theta(f_e)\, Q_w]_F \equiv \bar{c}_p(T_{i,s} - T_w) + Le\, h_d \times \zeta_w\, \alpha_{i,s}\, z_{F,w}\, I_\theta(f_e)_F \quad (43a)$$

$$[I_\theta(f_e)\, Q_w]_{eq} \equiv \bar{c}_p\,(T_{i,w} - T_w) + Le\, h_d\, \alpha_{i,w} \frac{\mathscr{I}_\theta(f_e)}{\mathscr{I}_z(f_e)} \quad (43b)$$

as the heat-transfer functions for chemically frozen or fully equilibrium shock layer flow, respectively. Then using equation (6) together with the fact that $H_s \simeq H_{i,e} \simeq H_{i,w}$, substitution of equations (34), (35) (with last term dropped) and (43b) into equation (18b) yields

$$\frac{I_\theta(f_e)\, Q_w}{[I_\theta(f_e)\, Q_w]_{eq}} = \frac{1 - \theta_w + (1 - Z)\, H_d[\mathscr{I}_\theta(f_e)/\mathscr{I}_z(f_e)] + \zeta_w\, z_{F,w}\, H_d\, Z\, I_\theta(f_e)}{1 - \theta_w + H_d + \left(\frac{\alpha_{i,w}}{\alpha_{i,s}}\right) Le\, H_d \left[\frac{\mathscr{I}_\theta(f_e)}{\mathscr{I}_z(f_e)} - 1\right]} \quad (44)$$

When $Le = 1$, the right-hand side of equation (44) can be shown to reduce to the simpler value $[H_\infty - H(0)]/(H_\infty - \bar{c}_p T_w)$ given by direct integration of the enthalpy form of the energy equation.

literature, evaluate Γ_i and ζ_w from equation (25) and (19) respectively, and calculate a first approximation for the post shock properties (including f_s and Re_s) assuming frozen flow across the shock without shock slip. (2) Upon selecting $f_e = f_i$ from Table 1, determine the nonequilibrium inviscid flow state $\alpha_{i,e}$, $T_{i,e}$ [and hence from equations (23) and (31) the values of $\mathscr{R}_{i,e}$ and Γ_b] according to the procedure outlined in the last paragraph of Section 3(a). (3) Now evaluate Ω_e, $I_z(f_e)$, $\mathscr{I}_{F,j}$ and $\mathscr{I}_f^d$ from the Appendix and $z_{f,w}$, r_d and Γ^* from equations (37), (40) and (41) respectively. (4) The key quantity Z may now be evaluated from either equation (39) or Fig. 4, from which

Table 1. Location of boundary layer edge for highly-cooled walls

P_R	0·50	0·70	1·00
f_e	4·48	3·38	2·19

4. APPLICATION OF THEORY

(a) *Calculation procedure*

To facilitate use of the present solution, it is desirable to outline the essential computational steps involved. Having specified the free stream conditions, body size, wall temperature, surface catalytic efficiency and the appropriate thermochemical properties of the gas such as shown in Table 2, one proceeds as follows. (1) Establish the equilibrium inviscid stagnation properties ($\rho_{i,w}$, β_i, etc.) from information available in the

Table 2. Parameters used in example calculations

$\bar{c}_p$	$= 4{\cdot}5\, R_m$
k_R'	$= 2{\cdot}59 \times 10^{14}\,(4500^\circ\mathrm{K})^-\ \mathrm{cm^6\ mole^{-2}\ s^{-1}}$
s	$= 1{\cdot}5$
ω	$= -1{\cdot}5$
A	$= \exp 4{\cdot}287$
T_D	$= 101\,276^\circ\mathrm{K}$
T_v	$= 3143^\circ\mathrm{K}$
h_d	$= 3{\cdot}183 \times 10^8\ \mathrm{ft^2/s^2}$
$\mathscr{I}_\theta(f_e)$	$= Le^{-0{\cdot}45}\, \mathscr{I}_Z(f_e)$
R_m	$= 3{\cdot}11 \times 10^3\ \mathrm{ft^2\ s^{-2}\ degK^{-1}}$
P_R	$= 0{\cdot}70$
Le	$= 1{\cdot}00$
R_B	$= 1\ \mathrm{ft}$
T_w	$= 1500^\circ\mathrm{K}$
V_∞	$= 26000\ \mathrm{ft/s}$
$\rho_R \mu_R$	$= \rho_s \mu_s$

the atom concentration at the wall can be calculated as $\alpha(0) = \alpha_{i,e}\, z_{f,w} Z$. Using the approximate value [7] $\mathscr{I}_\theta(f_e)/\mathscr{I}_z(f_e) = Le^{-0.45}$, the corresponding nonequilibrium heat-transfer ratio Q/Q_{eq} is then found from equation (44).

Following this procedure, it has been found that the application of the present solution to practical problems is rapid and straightforward. When the binary scaling principle governing the dissociation-dominated portion of the nonequilibrium flow regime is also used, a wide range of total enthalpy, Reynolds number and body surface conditions can be treated. In this connection, it is noted that an arbitrary degree of free stream dissociation may be included, provided that the state of such dissociation is consistent with our hypersonic strong shock assumption [24].

(b) *Results for nonequilibrium heat transfer*

A typical result of the present theory is illustrated in Fig. 5, where the stagnation point heat-transfer ratio Q/Q_{eq} is plotted versus altitude for a perfectly non-catalytic axisymmetric body with $R_b = 1$ ft flying at 26000 ft/s in the undissociated standard atmosphere, assuming $Le = 1$. (Values of the parameters assumed in the calculations, which correspond to reference [9], are indicated in Table 2.) To bring out the various physical effects involved, there is also indicated the result obtained assuming an equilibrium inviscid flow and that obtained by neglecting the inviscid reaction "carry-over" effect connected with the term r_d in equation (39). Shock-slip effects have not been included in these calculations in order to permit a direct comparison with the numerical results of Chung [9], who neglected these effects *a priori*. It is seen that the present theory agrees well with Chung throughout the nonequilibrium flow regime, underestimating the effect of shock layer reaction on heat transfer by no more than 10 per cent. It is noted, however, that this agreement is noticeably poorer when the explicit inviscid reaction "carry-over" effect is neglected, resulting in an increasing overestimate of heat transfer at the lower densities corresponding to dissociation rate-controlled shock layer flow.

The corresponding atom concentration at the edge of the boundary layer predicted by the present theory and Chung's calculations, respectively, is shown in Fig. 6. Here, also, there is good agreement between the two analyses.

As previously shown, the present theory embodies an account of shock-slip phenomena on the basis of the inviscid flow gradients, assuming an adiabatic shock. To evaluate the accuracy of approximation in this respect,

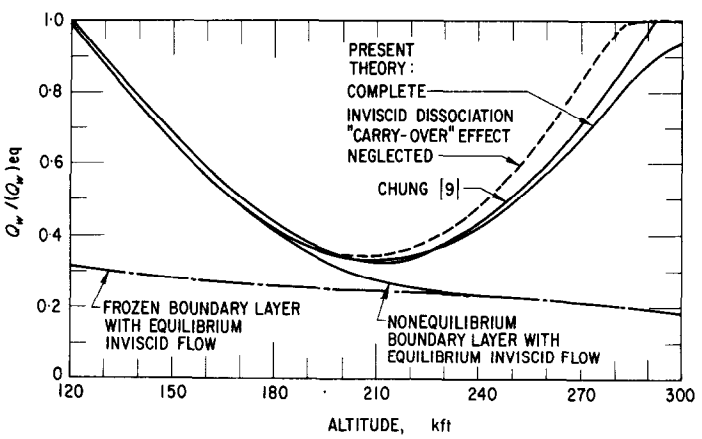

FIG. 5. Nonequilibrium stagnation point heat transfer; $V_\infty = 26000$ ft/s, $R_B = 1$ ft, $Le = 1$, non-catalytic surface.

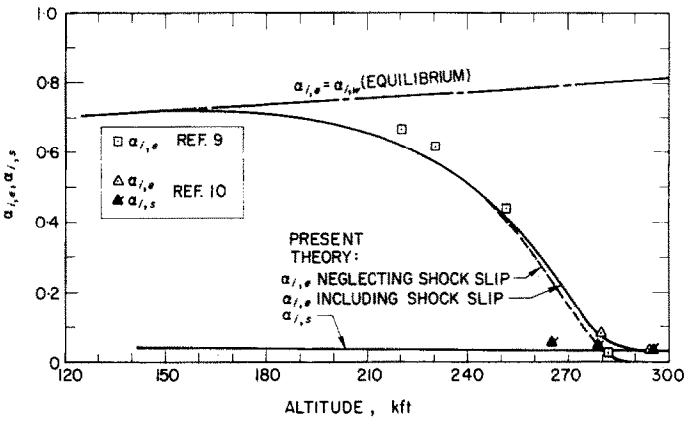

FIG. 6. Nonequilibrium atom concentrations.

Fig. 7 illustrates the heat-transfer curves obtained both with and without shock-slip effects included, along with Cheng's [10] numerical solution which included shock-slip. Since the latter results pertain to $Le = 1{\cdot}4$ and a slightly different pre-exponential temperature dependence for the dissociation rate than used here (namely, that appropriate to the Lighthill model), they have been normalized to Chung's results at $Re_s = 900$ to expose the shock-slip effects alone. It is seen that the predicted effect on heat transfer (due in this example entirely to concentration jump) agrees fairly well with the exact calculations. Equally good agreement is evident in Fig. 6 for the nonequilibrium atom concentrations at the edge of the boundary layer and immediately behind the shock.†

(c) *Effects of finite surface catalysis*

The effect of a non-vanishing surface catalycity on the nonequilibrium heat transfer results of Fig. 5 is shown in Fig. 8 as a function of the catalytic reaction parameter ζ_w. It is seen that the influence of gas phase reaction is very sensitive to the surface catalycity when the shock layer is appreciably out of equilibrium and significantly dissociated. This sensitivity is greatest when the boundary layer is chemically frozen while the inviscid flow is essentially in equilibrium; however, it persists well into the lower Reynolds number regime of completely dissociation rate-controlled flow.

In connection with these general results, it is of interest to indicate what actual degrees of surface catalycity and heat transfer can be expected for various surface materials. Accordingly, ζ_w and the corresponding heat transfer were evaluated as a function of altitude assuming $\gamma_w = 10^{-2}$ (typical of metallic oxides [25]), 10^{-3} and 10^{-4} (typical of glassy-type materials, such as pyrex [25]); the results are indicated on Fig. 8 by the dashed curves. It is seen that blunt bodies having a metallic-type surface behave as very nearly perfectly catalytic throughout most of the nonequilibrium flight regime in this example and consequently experience virtually the full equilibrium stagnation heating level regardless of altitude. Here, the body surface tends to act in a perfectly noncatalytic manner only at very high altitudes where little dissociation occurs in the shock layer. In sharp contrast, glassy-type surfaces having catalytic efficiencies of the order of 10^{-2} or less behave as though they were perfect noncatalysts under

† Note that at sufficiently low ambient density, the shock concentration jump is independent of altitude. This can be understood from equation (26), which shows that for negligible post-shock recombinations, $(\alpha_{i,s} - \alpha_\infty) \sim \Gamma_i R_{i,s} f_s^{-2} \sim p \rho_\infty^{-1} = \text{const.}$ at fixed ambient gas composition and velocity.

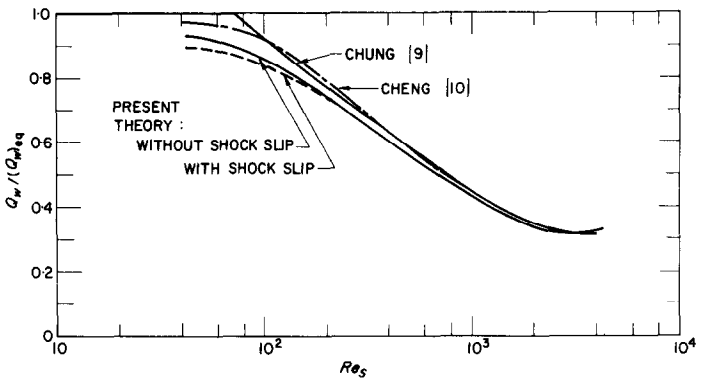

FIG. 7. Shock-slip effect on nonequilibrium heat transfer.

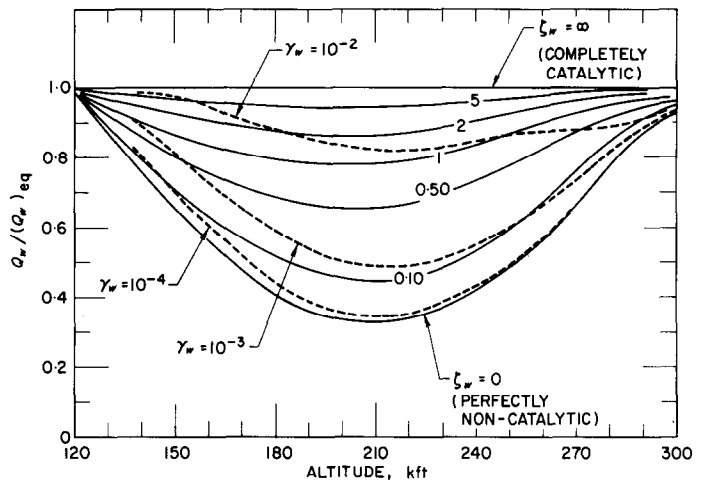

FIG. 8. Effect of surface catalycity on nonequilibrium heat transfer.

the same flight conditions. They therefore experience stagnation heat-transfer rates substantially lower than the equilibrium value throughout the altitude range 150–270 kft. Clearly, the choice of surface materials from the standpoint of their surface catalytic efficiency can have an important bearing on convective heating of hypervelocity vehicles that spend appreciable time at high altitudes. In this respect, current day ablation materials of glassy-like character would appear advantageous for reducing (as well as protecting against) the heat loads.

5. CONCLUSION

It has been shown that the problem of nonequilibrium viscous stagnation flow on blunt bodies over a wide range of practical conditions resides mainly in one basic flow regime. This regime, which extends down to $Re_s \gtrsim 100$, is a nonequilibrium vorticity interaction regime with a thick boundary layer and a reacting inviscid flow region near the shock. Approximate analytical solutions were obtained for both the inviscid and boundary layer regions, including an arbitrary surface catalycity and a first order account of shock slip effects assuming an adia-

batic bow shock. The resulting predictions of atom concentrations and heat transfer were found to be within 10 per cent of existing exact numerical solutions throughout the nonequilibrium flow regime.

The present theory completely describes the transition from recombination rate-controlled nonequilibrium boundary-layer behavior with an equilibrium-dissociated inviscid flow to dissociation rate-controlled, fully viscous shock layer flow with binary scaling at low Reynolds numbers. Immediate application is found in a related experimental study of nonequilibrium heat transfer being carried out at this laboratory using the catalytic probe [26], where measurements are made throughout the nonequilibrium shock layer flow regime. An equally important aspect of the present theory is that it permits comparatively simple yet accurate engineering calculations and so may be used for preliminary design analysis of hypervelocity vehicles. An example of this was given in Fig. 8, where it was shown that the choice of surface material from the standpoint of its catalytic efficiency can strongly affect the convective heating of such vehicles at high altitudes.

REFERENCES

1. J. A. FAY and F. R. RIDDELL, Theory of stagnation point heat transfer in dissociated air, *J. Aeronaut. Sci.* **25**, 73–85, 121 (1958).
2. P. M. CHUNG and A. D. ANDERSON, Heat transfer around blunt bodies with nonequilibrium boundary layers, *Proceedings of the* 1960 *Heat Transfer and Fluid Mechanics Institute*, pp. 150–162. Stanford University Press, California (1960).
3. J. A. MOORE and A. PALLONE, Similar solutions to the laminar boundary layer equations for nonequilibrium air, AVCO Corp. RAD TM-62-59 (July 1962).
4. F. G. BLOTTNER, Chemical nonequilibrium boundary layer, AIAA. Preprint 63-443 (August 1963).
5. P. M. CHUNG and S. W. LIU, Simultaneous gas-phase and surface atom recombination for stagnation boundary layer, *AIAA Jl* **1**, 929–931 (1962).
6. A. LINAN and I. DARIVA, Chemical nonequilibrium effects in hypersonic aerodynamics, Third International Congress on Aeronautical Science, Stockholm (August 1962).
7. G. R. INGER, Nonequilibrium stagnation point boundary layers with arbitrary surface catalycity, *AIAA Jl* **1**, 1776–1784 (1963).
8. D. E. ROSNER, Scale effects and correlations in nonequilibrium convective heat transfer, *AIAA Jl* **1**, 1550–1555 (1963).
9. P. M. CHUNG, Hypersonic viscous shock layer of nonequilibrium-dissociating gas, NASA R-109 (1961).
10. H. K. CHENG, The blunt body problem in hypersonic flow at low Reynolds number, IAS Paper 63-92 (January 1963).
11. F. J. STODDARD, Closed-form solutions for the hypersonic viscous shock layer with finite-rate chemistry, *Proceedings of the* 1963 *Heat Transfer and Fluid Mechanics Institute*, pp. 120–141. Stanford University Press, California (1963).
12. H. K. CHENG, Hypersonic shock-layer theory of the stagnation region at low Reynolds number, *Proceedings of the* 1961 *Heat Transfer and Fluid Mechanics Institute*, p. 161. Stanford University Press, California (1962). Also see Cornell Aero. Lab. Report AF-1285-A-7 (April 1961).
13. H. K. CHENG and A. L. CHANG, Stagnation region in rarefied high Mach number flow, *AIAA Jl* **1**, 231–233 (1963).
14. H. HOSHIZAKI, S. NEICE and K. K. CHEN, Stagnation point heat transfer rates at low Reynolds numbers, IAS Paper 60–68 (June 1960).
15. L. GOLDBERG and S. SCALA, Mass transfer in the hypersonic low Reynolds number viscous layer, IAS Paper 62-80 (January 1962).
16. G. R. INGER, Nonequilibrium hypersonic stagnation flow at low Reynolds numbers, Aerospace Corp. SSD-TDR-64-118 (September 1964).
17. J. D. BUCKMASTER, The effects of ambient dissociation on frozen hypersonic stagnation flow, AEDC-TDR-64-142 (Cornell Aero. Lab.) (June 1964).
18. W. D. HAYES and R. F. PROBSTEIN, *Hypersonic Flow Theory*, p. 371. Academic Press, New York (1959).
19. W. E. GIBSON and A. SOWYRDA, An analysis of nonequilibrium inviscid flows, AEDC TRD-62-172 (August 1962).
20. M. J. LIGHTHILL, Dynamics of a dissociating gas; Part I, Equilibrium flow, *J. Fluid Mech.* **2**, 12 (1957).
21. W. E. GIBSON, Dissociation scaling for nonequilibrium blunt-nose flows, *ARS Jl.* **32**, 285–287 (1962).
22. C. B. COHEN and E. RESHOTKO, Similar solutions for the compressible laminar boundary layer with heat transfer and pressure gradient, NACA Report 1293 (1956).
23. P. DERIENZO and J. A. PALLONE, Convective stagnation point heating for reentry speeds up to 70000 ft./sec. including effects of large blowing rates, AVCO RAD (Wilmington, Mass.) TM-65-58 (January 1965).
24. G. R. INGER, Viscous and inviscid stagnation flow in dissociated hypervelocity free streams, *Proceedings of the* 1962 *Heat Transfer and Fluid Mechanics Institute*, pp. 95–108. Stanford University Press, California (1962).
25. R. J. GOULARD, On catalytic recombination rates in hypersonic stagnation heat transfer, *Jet Propul.* **28**, 737–745 (1958).
26. R. A. HARTUNIAN and W. P. THOMPSON, Nonequilibrium stagnation point heat transfer including surface catalysis, AIAA Preprint 63-464 (August 1963).

APPENDIX

Numerical values of the integral functions defined by equations (36) have been computed for a wide range of the relevant fluid-mechanical and thermochemical parameters using boundary-layer velocity profiles including vorticity-interaction effects [12]. Under the conditions $T_w/T_{i,w} \leqslant 0{\cdot}30$ and $\Omega_e < 1$, it was found that

$$I_z(f_e) \simeq [0{\cdot}47\, Sc^{1/3}(1 + 0{\cdot}50\,\Omega_e - 0{\cdot}11\,\Omega_e^2)]^{-1} \qquad \text{(A-1)}$$

where

$$\Omega_e = \frac{[(V_\infty/\beta_i R_b)^2 - (\rho_{i,w}/\rho_{i,e})][1 - (1+v)(\rho_{i,s}/\rho_\infty)(\rho_R\mu_R/\rho_s\mu_s\, Re_s)]}{\{(\rho_s\mu_s/\rho_R\mu_R)[4\rho_\infty/(1+v)\,\rho_s](V_\infty/\beta_i R_b)\, Re_s\}^{\frac{1}{2}}} \qquad \text{(A-2)}$$

is a vorticity-interaction parameter similar to Cheng's, here generalized to include inviscid nonequilibrium reaction and shock velocity slip effects. Correspondingly, the reaction rate integrals $\mathscr{I}_{F_{1,2,3}}$ and $\mathscr{I}_F^d$ are given by

$$\mathscr{I}_{F_j} = (1 + 0{\cdot}50\,\Omega_e - 0{\cdot}11\,\Omega_e^1)^{-N_j}\,[\mathscr{I}_{Z_F}(\infty)]_j \qquad (j = 1, 2, 3) \qquad \text{(A-3)}$$

$$\mathscr{I}_F^d = \int_0^{\eta(f_e)} \exp\left(-Sc\int_0^\eta f\,d\eta\right)\left\{\int_0^\eta \exp\left(Sc\int_0^\eta f\,d\eta\right)\theta_F^{\omega+s-2}\exp\left[-(\theta_d/\theta_F)+\theta_d\right]d\eta\right\}d\eta \qquad \text{(A-4)}$$

where $N_1 = 1{\cdot}35$, $N_2 = 0{\cdot}36$ and $N_3 = -0{\cdot}66$, respectively. The $[\mathscr{I}_{Z,F}{}^{(\infty)}]_j$ are precisely the recombination rate integral functions of θ_d, θ_w and ω given in references (7) and (16). The integral $\mathscr{I}_F^d$ is plotted as a function of θ_w and θ_d in Fig. 9 for different values of the parameter $\omega + s$. For convenience, a tabulation of some representative values of all four reaction rate integrals is given in Table 3.

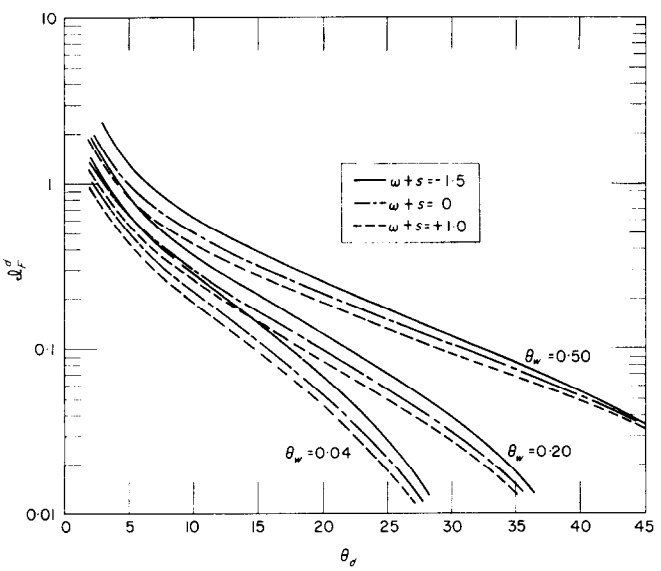

FIG. 9. Boundary layer dissociation rate integral $\mathscr{I}(d/F)$.

Table 3. Reaction rate integral functions for $Sc = 0{\cdot}50$, $\omega = -1{\cdot}5$, $S = 0$

θ_w	$\mathscr{I}_{z,F(\infty)_1}$ $\theta_D = 5$	$\theta_D = 15$	$\theta_D = 25$	$\mathscr{I}_{z,F(\infty)_2}$ $\theta_D = 5$	$\theta_D = 15$	$\theta_D = 25$	$\mathscr{I}_{z,F(\infty)_3}$ $\theta_D = 5$	$\theta_D = 15$	$\theta_D = 25$	$\mathscr{I}_F^A$ $\theta_D = 5$	$\theta_D = 15$	$\theta_D = 25$
0·04	$8{\cdot}2 \times 10^3$	$8{\cdot}2 \times 10^3$	$8{\cdot}2 \times 10^3$	$1{\cdot}8 \times 10^2$	$1{\cdot}9 \times 10^2$	2×10^2	$1{\cdot}4 \times 10$	$1{\cdot}5 \times 10$	$1{\cdot}6 \times 10$	$6{\cdot}37 \times 10^{-1}$	$1{\cdot}43 \times 10^{-1}$	$2{\cdot}86 \times 10^{-2}$
0·10	$8{\cdot}4 \times 10^2$	$8{\cdot}4 \times 10^2$	$8{\cdot}4 \times 10^2$	$5{\cdot}2 \times 10$	$5{\cdot}6 \times 10$	$6{\cdot}0 \times 10$	5·9	6·5	7·2	$7{\cdot}1 \times 10^{-1}$	$1{\cdot}65 \times 10^{-1}$	$4{\cdot}95 \times 10^{-2}$
0·20	$1{\cdot}6 \times 10^2$	$1{\cdot}6 \times 10^2$	$1{\cdot}6 \times 10^2$	$1{\cdot}7 \times 10$	$1{\cdot}83 \times 10$	$2{\cdot}0 \times 10$	3·0	3·5	4·0	$8{\cdot}5 \times 10^{-1}$	$2{\cdot}10 \times 10^{-1}$	$7{\cdot}40 \times 10^{-2}$
0·35	$4{\cdot}1 \times 10$	$4{\cdot}2 \times 10$	$4{\cdot}3 \times 10$	6·2	7·6	8·7	1·10	1·98	2·42	1·05	$2{\cdot}82 \times 10^{-1}$	$1{\cdot}18 \times 10^{-1}$
0·50	$1{\cdot}64 \times 10$	$1{\cdot}75 \times 10$	$1{\cdot}90 \times 10$	3·2	5·3	5·4				1·32	$3{\cdot}82 \times 10^{-1}$	$1{\cdot}73 \times 10^{-1}$

Résumé—On considère un écoulement avec dissociation au point d'arrêt sur des corps arrondis fortement refroidis placés dans un écoulement hypersonique d'air ou de gaz diatomique, en tenant compte des effets de nombre de Reynolds et d'une réaction chimique à travers la couche de choc. On suppose que la vitesse de recombinaison atomique sur la surface est arbitraire. En se basant sur le modèle de Cheng d'une couche de choc mince en régime continu, on montre que, dans de nombreuses applications, des effets importants dus à la réaction en phase gazeuse se produisent dans unrégime d'intéraction aveç un écoulement rotationnel en non-équilibre, ce qui implique un passage du contrôle par la vitesse de recombinaison au contrôle par la vitesse de dissociation. On donne une solution analytique approchée pour ce régime qui prédit des concentrations atomiques et un transport de chaleur en non-équilibre à 10 pour cent près des solutions numériques exactes jusqu'à des nombres de Reynolds de couche de choc de 100.

Zusammenfassung—Die Staupunktströmung mit Dissoziation an stark gekühlten stumpfen Körpern in einem Luft- oder zweiatomigen Gasstrom von Hyperschallgeschwindigkeit wird untersucht. Einflüsse kleiner Reynoldszahlen und chemische Nichtgleichgewichtsreaktionen innerhalb der StossSchicht sind ebenfalls berücksichtigt. Eine beliebige Geschwindigkeit der Staurekombination an der Oberfläche ist zugelassen. Auf Grund des Kontinuummodells dünner StossSchicht von Cheng wird gezeigt, dass in vielen Anwendungen die kennzeichnenden Einflüsse der Gasphasenreaktion in einem verallgemeinerten Strömungsregime mit Wirbelwechselwirkung im Ungleichgewicht auftreten, einschliesslich des Übergangs vom rekombinations- zum dissoziationskontrollierten Verhalten. Eine für dieses Regime angegebene analytische Näherungslösung gestattet Atomkonzentrationen und den Wärmeübergang im Ungleichgewicht mit weniger als 10 prozent Abweichung von exakten numerischen Lösungen zu ermitteln, für Reynoldszahlen (StossSchicht) bis herab zu 100.

Аннотация—Рассматривается обтекание сильно охлаждаемых затупленных тел сверхзвуковым потоком воздуха или двухатомного газа в окрестности критической точки при низких числах Рейнольдса и неравновесной химической реакции в ударном слое. Допускается произвольная скорость рекомбинации атомов на поверхности. На основании модели Ченга непрерывного тонкого ударного слоя показано, что во многих случаях реакции в газовой фазе значительно влияют на режим обобщенного неравновесного завихренного потока, включая переход от режима, определяемого рекомбинацией, к режиму, определяемому скоростью диссоциации. Дается приближенное аналитическое решение для этого режима, которое позволяет рассчитать концентрацию атомов и неравновесный перенос тепла с точностью до 10% по сравнению с точными численными решениями при числах Рейнольдса для ударного слоя, равных 100.